

The Local Spin Structure of Large Spin Fermions

Tin-Lun Ho^{1,2*} and Biao Huang^{1†}

¹*Department of Physics, The Ohio State University, Columbus, OH 43210, USA*

²*Institute for Advanced Study, Tsinghua University, Beijing 100084, China*

(Dated: April 8, 2022)

We show that large spin fermions have very rich spin structures. The local spin order of a spin- f Fermi gas is a linear combination of $2f$ (particle-hole) angular momentum states, $L = 1, \dots, 2f$. $L = 1, 2$ represent ferromagnetic and nematic spin order, while $L \geq 3$ are higher spin orders that have no analog in spin-1/2 systems. Each L spin sector is characterized as L pairs of antipodal points on a sphere. Model calculations show that some of these spin-orders have the symmetry of Platonic solid, and many of them have non-abelian line defects.

I. INTRODUCTION

Prior to the discovery of Bose-Einstein condensates, the only quantum liquids realized experimentally are the electron liquids in solids, and the low temperature phases of liquid ⁴He and ³He. All these systems are made up of spin-1/2 fermions (like electrons and ³He atoms), or spin-0 bosons (⁴He atoms). Recent advances in the cooling of atomic gases, however, have created the exciting opportunities of studying high spin quantum fluids. The spins of atomic bosons can range from $f = 1, 2$ (⁸⁷Rb bosons) to $f = 8$ (¹⁶²Dy bosons)[1], and the spin of atomic fermions can be as high as $f = 9/2$ (⁴⁰K) and $f = 21/2$ (¹⁶¹Dy)[2]. Theoretical generalizations of the Bose-Einstein condensate and fermion pair superfluids to high spin particles have been made about a decade ago [3, 4].

While there are many experiments on large spin Bose condensates (or spinor condensates), experiments on large spin fermions are still at their infancy. At present, there is no realization of the superfluid phases of large spin fermions because of their very low transition temperatures. On the other hand, scatterings in different angular momentum channel and dipolar effects can lead to non-trivial spin structures in the normal state, which may be realized at higher temperatures. These scattering lengths in various spin channels can be measured using techniques in ref.[5–7]. As we shall see, these scattering lengths can lead to a great variety of spin structures in the normal state, most of which do not have analogs in solid state systems.

The possibility of rich spin structures for high spin fermions has already been illustrated in the cases of spin-3/2 fermions [8][10], spin-9/2 ⁴⁰K experiments[5–7], and alkali earth fermions with SU(N) symmetry[9]. The case of spin-3/2 fermions is very illuminating. By simply changing the spin value from 1/2 to 3/2, the system immediately gains a rich SO(5) symmetry. In this paper, we shall discuss the spin structure of spin- f fermions in the normal state by analyzing their single particle density matrices. We shall show that these density matrices can be decomposed into different angular momentum components, $L = 0, 1, \dots, 2f$ made up of a particle and a hole. We then show that each L -component can be represented by L pairs of antipodal points (or Majorana points)

on a sphere. From the single particle density matrix, one can see that the $L = 0$ component is the average density, and the $L > 1$ components describe the spin structure of the system. The entire spin structure is then specified by a sequence of $2f$ spheres with $1, 2, \dots, 2f$ pairs of antipodal Majorana points respectively. To illustrate the special properties of these spin structures, we shall study the class of inert states [11] which are robust against perturbations. We show that many of these inert states have the symmetry of Platonic solids and will have non-abelian line defects. Furthermore, we shall perform mean field calculations to demonstrate the emergence of some of these inert states.

II. SYMMETRY CLASSIFICATIONS

For spin- f bosons, its condensate (known as spinor condensates) is a $(2f + 1)$ component vector $\Psi_m(\mathbf{r}) = \langle \hat{\psi}_m(\mathbf{r}) \rangle$, $m = f, f - 1, \dots, -f$ [3], where $\hat{\psi}_m(\mathbf{r})$ is the field operator that destroys a particle with spin component m . For fermion superfluids made up of pairs of total angular momentum F , its order parameter also transforms like that of a spin- F spinor condensate[4]. In this work, we focus on the local spin order of a Fermi gas, which is contained in the single particle density matrix $\rho_{m_1 m_2} = \langle \hat{\rho}_{m_1 m_2} \rangle$,

$$\rho_{m_1 m_2}(\mathbf{r}) = \langle \hat{\psi}_{m_2}^\dagger(\mathbf{r}) \hat{\psi}_{m_1}(\mathbf{r}) \rangle. \quad (1)$$

For large spin systems where dipolar effects are important, ρ can acquire spatial variations even in equilibrium. For simplicity, we shall from now on suppress the spatial coordinate until they need to be made explicit.

Under a spin rotation θ , the field operator and the density matrix transform as

$$\hat{\psi}_m \rightarrow D_{mm'}^{(f)}(\theta) \hat{\psi}_{m'}, \quad (2)$$

$$\rho_{m_1 m_2} \rightarrow D_{m_1 m_3}^{(f)}(\theta) \rho_{m_3 m_4} D_{m_4 m_2}^{(f)\dagger}(\theta), \quad (3)$$

where repeated indices are summed over. Here we employ the rotation matrix $D_{mm'}^{(f)}(\theta) = \langle f m | e^{-i\theta \cdot \mathbf{F}} | f m' \rangle$ with the hermitian conjugate $D_{mm'}^{(f)\dagger}(\theta) = \langle f m | e^{i\theta \cdot \mathbf{F}} | f m' \rangle$. \mathbf{F} is the spin operator for spin- f particles and $|f m\rangle$ is the eigenstate of (\mathbf{F}^2, F_z) . To sort out the spin structure of $\rho_{m_1 m_2}$, we decompose it in terms of tensor operators of different angular momenta (made up

* ho@mps.ohio-state.edu

† phys.huang.biao@gmail.com

of a particle-hole pair). This is achieved by noting that the $(2f+1) \times (2f+1)$ matrix,

$$\left(\mathcal{Y}_M^{(L)}\right)_{m_1 m_2} \equiv \sqrt{\frac{2L+1}{2f+1}} \langle f m_1 | LM; f m_2 \rangle, \quad (4)$$

where $\langle f m_1 | LM; f m_2 \rangle$ is the Clebsch-Gordon coefficient, transforms under rotation as

$$D_{m_1 m_2}^{(f)}(\boldsymbol{\theta}) \left(\mathcal{Y}_M^{(L)}\right)_{m_2 m_3} D_{m_3 m_4}^{(f)\dagger}(\boldsymbol{\theta}) = \sum_{M'} \left(\mathcal{Y}_{M'}^{(L)}\right)_{m_1 m_4} D_{M'M}^{(L)}(\boldsymbol{\theta}). \quad (5)$$

Thus, $(\mathcal{Y}_M^{(L)})_{m_1 m_2}$ is a tensor operator [12] (with angular momentum L) in the spin- f space. We can then expand $\rho_{m_1 m_2}$ as

$$\rho_{m_1 m_2} = \sum_{L=0}^{2f} \sum_{M=-L}^L \Phi_M^{(L)} (\mathcal{Y}_M^{(L)})_{m_1 m_2}. \quad (6)$$

To simplify notation, we will sometimes omit the indices $(m_1 m_2)$ for $(\mathcal{Y}_M^{(L)})_{m_1 m_2}$ and $\rho_{m_1 m_2}$, and treat these matrices as $\mathcal{Y}_M^{(L)}$ and ρ . Since the Clebsch-Gordon coefficients are real numbers, so is $(\mathcal{Y}_M^{(L)})_{m_1 m_2}$. That means $\mathcal{Y}_M^{(L)\dagger} = \mathcal{Y}_M^{(L)T}$, where \dagger and T means hermitian conjugate and transpose of the matrix. Since the Clebsch-Gordon coefficients satisfies [12],

$$\mathcal{Y}_M^{(L)\dagger} = (-1)^M \mathcal{Y}_{-M}^{(L)}, \quad \text{Tr} \mathcal{Y}_M^{(L)} \mathcal{Y}_{M'}^{(L)\dagger} = \delta_{LL'} \delta_{MM'}. \quad (7)$$

we have

$$\Phi_M^{(L)} = \text{Tr}(\rho \mathcal{Y}_M^{(L)\dagger}). \quad (8)$$

From the rotational properties in Eqn (3) and (5), it is easy to show that the vector

$$\Phi^{(L)} \equiv (\Phi_{-L}^{(L)}, \dots, \Phi_L^{(L)})^T \quad (9)$$

transforms as a spin- L vector in spin space,

$$\Phi_M^{(L)} \rightarrow \Phi_M'^{(L)} = \sum_{M'} D_{MM'}^{(L)} \Phi_{M'}^{(L)}. \quad (10)$$

Another convenient way to represent this transformation property is to regard $\Phi_M^{(L)}$'s as the expansion coefficients of a abstract spin state $|\Phi^{(L)}\rangle$ in the angular momentum basis $|L, M\rangle$,

$$|\Phi^{(L)}\rangle = \sum_{M=-L}^L \Phi_M^{(L)} |LM\rangle. \quad (11)$$

The rotation property of $|\Phi^{(L)}\rangle$ immediately gives Eqn.(10). Note that not all $\Phi_M^{(L)}$ in $\Phi^{(L)}$ are independent. The fact that ρ is hermitian implies that

$$\Phi_M^{(L)*} = (-1)^M \Phi_{-M}^{(L)}. \quad (12)$$

This means $\Phi^{(L)}$ is specified by $2L+1$ independent real variables.

Finally, taking the trace of the expansion in Eqn.(6), we have

$$\Phi^{(0)} = n/(2f+1). \quad (13)$$

where we have made use of the fact that

$$\text{Tr} \mathcal{Y}_M^{(L)} = 0, \quad \text{for } L \geq 1. \quad (14)$$

To show Eq.(14), we take the Trace of Eqn.(5). This gives $\text{Tr} \mathcal{Y}_M^{(L)} = \text{Tr} \mathcal{Y}_{M'}^{(L)} D_{M'M}^{(L)}(\boldsymbol{\theta})$ for all $L \geq 1$ and all $\boldsymbol{\theta}$, which can only be satisfied if Eqn.(14) is valid. Because of Eqn.(13), one sees that the non-trivial spin structures are given by the traceless part of ρ ,

$$\tilde{\rho}_{mn} \equiv \rho_{mn} - \frac{n}{2f+1} \delta_{mn}. \quad (15)$$

Although $\Phi^{(L)}$ is formally similar to a spin- L spinor condensate, it has very different meaning. From Wigner-Eckart theorem, we note that $\mathcal{Y}_M^{(L)}$ is proportional to a product of L spin operators \mathbf{F} in spin- f space. Thus, $\Phi^{(1)}$ and $\Phi^{(2)}$ are proportional to a single and two \mathbf{F} operators respectively, and thus represent ferromagnetic and nematic order respectively in spin- f space. The vectors $\Phi^{(L)}$ for $L \geq 1$ will be referred to as the L -th spin order of the system, $L = 1, 2, \dots$, which are all contained in the traceless part of $\tilde{\rho}$.

To gain further insight, we express each $\Phi^{(L)}$ in Majorana representation as a set of $2L$ points (referred to as Majorana points) on the unit sphere S_2 [13–15]. To accomplish it, we use the Schwinger bosons representation of angular momentum states,

$$|LM\rangle = \frac{a^{\dagger L+M} b^{\dagger L-M}}{\sqrt{(L+M)!(L-M)!}} |0\rangle, \quad (16)$$

where a and b are boson operators, and $(a, b)^T$ transform as a spin-1/2 spinor [16]. A general state of the form Eqn.(11) can then be factorized as

$$|\Phi^{(L)}\rangle = \lambda^{(L)} \prod_{i=1}^{2L} (u_i^{(L)} a^\dagger + v_i^{(L)} b^\dagger) |0\rangle, \quad (17)$$

where $\lambda^{(L)}$ is a constant, and $\zeta_i^{(L)} \equiv (u_i^{(L)}, v_i^{(L)})^T$ is a normalized spinor

$$|u_i^{(L)}|^2 + |v_i^{(L)}|^2 = 1. \quad (18)$$

Eqn.(17) follows from the fundamental theorem of algebra which implies a homogenous polynomial $\mathcal{P}(x, y) = \sum_{M=-L}^L \alpha_M x^{L+M} y^{L-M}$ can be factorized to $2L$ linear terms $\mathcal{P}(x, y) = \lambda \prod_{i=1}^{2L} (u_i x + v_i y)$.

To simplify notations, we shall suppress the superscript $^{(L)}$ when we discuss a specific L component. It will be reinstated when needed. Using the standard representation for a spinor

$$\zeta = (u, v)^T \equiv \left(\cos \frac{\theta}{2} e^{-i\phi/2}, \sin \frac{\theta}{2} e^{i\phi/2} \right)^T e^{i\chi/2}, \quad (19)$$

we have

$$\zeta^\dagger \vec{\sigma} \zeta = \hat{\mathbf{n}} = \cos\theta \hat{\mathbf{z}} + \sin\theta (\cos\phi \hat{\mathbf{x}} + \sin\phi \hat{\mathbf{y}}). \quad (20)$$

Hence each ζ_i in Eqn.(17) can be represented as a point on the unit sphere S_2 in the direction $\hat{\mathbf{n}}_i$ with polar angle (θ_i, ϕ_i) . Note that all the phases χ_i are absorbed into the constant λ .

However, not all $\hat{\mathbf{n}}_i$'s are independent, as Eqn.(12) implies that Eqn.(17) can be rewritten as

$$\begin{aligned} |\Phi^{(L)}\rangle &= \sum_{M=-L}^L \frac{\Phi_M^{(L)*}}{\sqrt{(L+M)!(L-M)!}} b^{\dagger L+M} (-a^\dagger)^{L-M} |0\rangle \\ &= \lambda^* \prod_{i=1}^{2L} (u_i^* b^\dagger - v_i^* a^\dagger) |0\rangle \end{aligned} \quad (21)$$

where we have suppressed the superscript (L) . Eqn.(21) shows that the spinors ζ_i in Eqn.(17) must be accompanied by its time reversed partner $-i\sigma_2 \zeta_i^* = (-v_i^*, u_i^*)$. Therefore, the $2L$ vectors $\hat{\mathbf{n}}_i$ must appear in antipodal pairs $(\hat{\mathbf{n}}_i, -\hat{\mathbf{n}}_i) \equiv [\hat{\mathbf{n}}_i]$. It is then sufficient to represent each pair by only one of its members. The presence of antipodal pairs implies Eqn.(17) is of the form

$$\begin{aligned} |\Phi^{(L)}\rangle &= \lambda^{(L)} \prod_{i=1}^L (-u_i v_i^* a^{\dagger 2} + (|u_i|^2 - |v_i|^2) a^\dagger b^\dagger + u_i^* v_i b^{\dagger 2}) |0\rangle \\ &= \frac{\lambda^{(L)}}{2} \prod_{i=1}^L (\sin \theta_i e^{i\phi_i} b^{\dagger 2} - \sin \theta_i e^{-i\phi_i} a^{\dagger 2} + \cos_i \theta_i a^\dagger b^\dagger) |0\rangle \end{aligned} \quad (22)$$

with $\lambda^{(L)*} = \lambda^{(L)}$ because of Eqn.(12). The $(2L+1)$ real variables of $\Phi^{(L)}$ is now represented by the L unit vectors $\hat{\mathbf{n}}_i$ and a real number $\lambda^{(L)}$. In equilibrium, different $\lambda^{(L)}$'s are correlated to minimize the energy.

In summary, we have decomposed the non-trivial traceless part of the density matrix $\tilde{\rho}_{m_1 m_2}(\mathbf{r})$, which represent local spin order into various spin- L vectors $\Phi^{(L)}$, where $L = 1, 2, \dots, 2f$. Each $\Phi^{(L)}$ is represented by L antipodal pairs of points on a spherical surface, whose radius $\lambda^{(L)}$ represents the strength of the L -sector of spin order. In the following, we discuss the properties of the local spin order in each L -sector.

III. TOPOLOGICAL DEFECTS AND SPIN TEXTURE OF DIFFERENT SPIN ORDER SECTORS

For $L = 1$, the ferromagnetic order, there is only one pair of Majorana points $[\hat{\mathbf{n}}]$. (See Fig. 1(i)). Since $\hat{\mathbf{n}}$ can be in any direction, the configurational space is the unit sphere S_2 . Note that $[\hat{\mathbf{n}}]$ and $[-\hat{\mathbf{n}}]$ are distinct because $|\Phi^{(1)}\rangle$ becomes $-|\Phi^{(1)}\rangle$ as $\hat{\mathbf{n}}$ changes continuously to $-\hat{\mathbf{n}}$ [18]. Since the first homotopy group of S_2 is trivial, $(\pi_1(S_2) = 0)$, the vector field $\{\Phi_M^{(1)}(\mathbf{r})\}$ has no topologically stable line defects[20].

For $L = 2$, the nematic order, there are two Majorana pairs $[\hat{\mathbf{n}}][\hat{\mathbf{m}}]$. If $\hat{\mathbf{n}} = \pm\hat{\mathbf{m}}$, the system is uniaxial nematics characterized by a single antipodal pair on the unit sphere with each pole doubly occupied. (See Fig.1(ii)). Unlike $L = 1$, where $[\hat{\mathbf{n}}]$ and $[-\hat{\mathbf{n}}]$ are distinct, the states $[\hat{\mathbf{n}}][\hat{\mathbf{n}}]$ and $[-\hat{\mathbf{n}}][-\hat{\mathbf{n}}]$ are identical, as they correspond to the same

state $|\Phi^{(2)}\rangle = \lambda(u a^\dagger + v b^\dagger)^2 (-v^* a^\dagger + u^* b^\dagger)^2 |0\rangle$. (Note that $([\hat{\mathbf{n}}][-\hat{\mathbf{n}}] = -[\hat{\mathbf{n}}][\hat{\mathbf{n}}])$. The configuration space is therefore S_2 with antipodal points identified, which is the projected space P_2 . Since $\pi_1(P_2) = Z_2$, there is only one type of nontrivial line defect. If $\hat{\mathbf{n}} \neq \pm\hat{\mathbf{m}}$, it is straightforward to show that $|\Phi^{(2)}\rangle$ is unchanged only under a π rotation along the orthogonal axes $\hat{\mathbf{n}} \times \hat{\mathbf{m}}$, $\hat{\mathbf{n}} + \hat{\mathbf{m}}$, and $\hat{\mathbf{n}} - \hat{\mathbf{m}}$. (See [19] and see Fig. 1(iii)). The system is therefore a bi-axial nematics, and has nonabelian line defects[20].

For $L \geq 3$, there will be more pairs of Majorana points. A simple case is that all pairs locate at the same position, as what happens for uniaxial nematics. The discussions above show that for odd and even L , the configuration space is S_2 and P_2 respectively. In general, the pairs of points can distribute arbitrarily, forming the vertices of an irregular polygon, as those in Fig. 1 (e). The fact that *the Majorana points must appear in antipodal pairs forbids the polygon to have tetrahedral symmetry*, as shown in (Fig.1 (iv)). This is different from the situation in bosonic spinor condensates where tetrahedral symmetry is allowed in the case when spin $S \geq 2$ [14].

Of particular interests are the cases when the Majorana points are distributed in high symmetry, such as the Platonic solids shown in Fig. (c) (d) (f) (g), which are cube, octahedron, isocahedron, and dodecahedron respectively. The symmetry groups of (c) and (d) is the octahedral group O , and that for (f) and (g) is isocahedral group Y . These states belong to the class of "inert states" whose structures (i.e. distribution of Majorana points) are independent of interaction parameters[17]. These states, if present, must therefore occupy a finite region in parameter space, and have a good chance of being observed. We show in the next section through a mean field calculation that all these Platonic solids states can arise from spin exchange interaction[3].

As mentioned before, the spin order is specified by the set of vectors $\{\Phi^{(L)}\}$ with $L = 1, 2, \dots, 2f$. In general, when dipolar interaction is taken into account, these vectors (and their corresponding Majorana points in S_2) will vary in space, forming a spin texture in each L -sector. The general behavior of these spin textures $\{\Phi^{(L)}(\mathbf{r})\}$ is illustrated in Figure 1 (1-7) for the case of $f = 7/2$. The figure displays the spin orders $|\Phi^{(L)}(x)\rangle$ along a loop C in real space, which can be represented as a straight line along x with end points identified. The entire set of spin order $\{\Phi^{(L)}(x), L = 1, 2, \dots, 2f\}$ is represented as an array of $2f$ spherical surfaces with radius $|\lambda^{(L)}(x)|$ and L pairs of antipodal Majorana points. One can recall that the spin texture in spin-1/2 systems corresponds to a rotation of a vector in space; the direction of the vector designates the local spin order (\mathbf{S}) . In comparison, the spin textures in higher L -sector of the spin order correspond to the rotation (or even deformation) of a polygon in space. As long as $\lambda^{(L)}(x) \neq 0$ and different Majorana pairs do not merge as on traverses the loop C , each L sector can have its own line defects.

IV. ENERGETIC CONSIDERATIONS AND PLATONIC SOLID INERT STATES

Next, we discuss how interaction effects give rise to the spin order discussed above. We shall consider a general short

range spin-exchange interaction between fermions[3]. Such a description has been shown to be effective in recent experi-

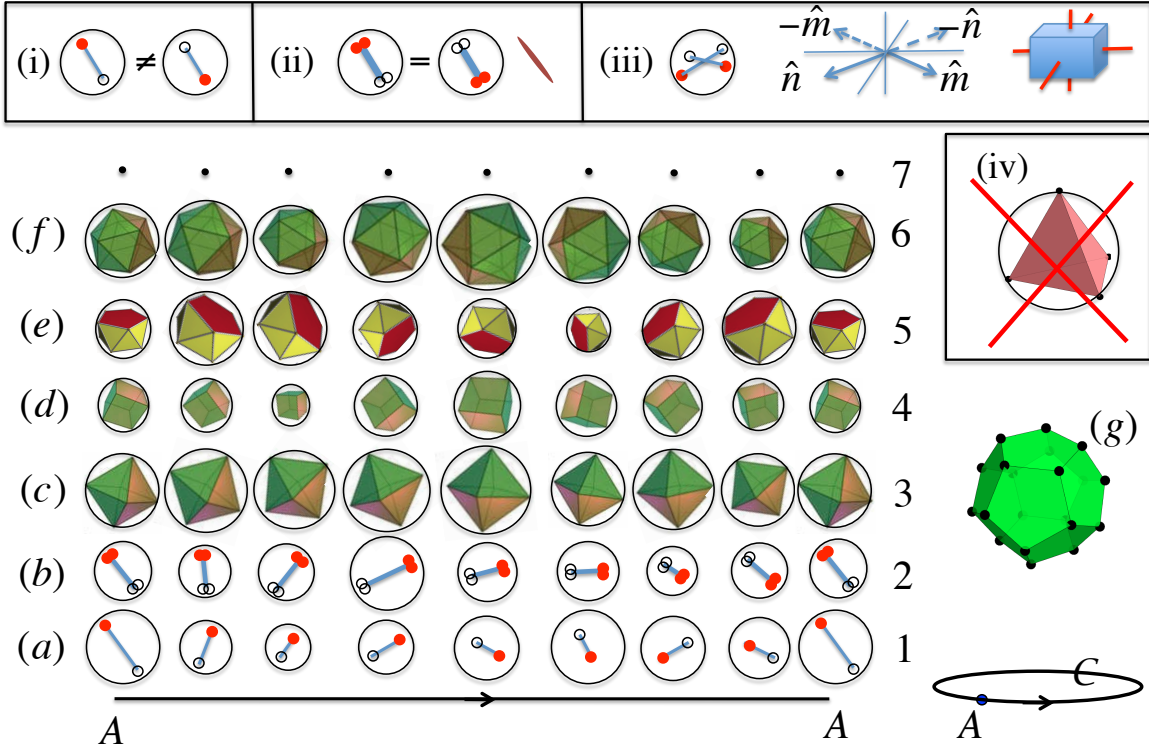


FIG. 1. Inset (i): Ferromagnetic order $\Phi^{(1)}$ represented the Majorana pair $[\hat{\mathbf{n}}] \equiv (\hat{\mathbf{n}}, -\hat{\mathbf{n}})$. $[\hat{\mathbf{n}}]$ and $[-\hat{\mathbf{n}}]$ are distinct. Inset (ii) : Uniaxial nematic state $\Phi^{(2)}$ represented by two identical Majorana pairs: It has the symmetry of a rod. $[\hat{\mathbf{n}}][\hat{\mathbf{n}}]$ and $[-\hat{\mathbf{n}}][-\hat{\mathbf{n}}]$ are identical. (iii) Biaxial nematic state $\Phi^{(2)}$ with two distinct Majorana pairs: The quantum state is invariant under π rotation about $\hat{\mathbf{n}} \times \hat{\mathbf{m}}$, $\hat{\mathbf{n}} + \hat{\mathbf{m}}$, $\hat{\mathbf{n}} - \hat{\mathbf{m}}$. It has the symmetry of a brick with different edge lengths. Inset (iv): The Majorana points can not form a tetrahedron because its vertices do not form antipodal pairs. The numerals (1, 2, ..7) denote the spin order ($\Phi^{(1)}, \Phi^{(2)}, \dots, \Phi^{(7)}$) of a spin $f = 7/2$ Fermi gas along the loop C in real space. $\Phi_M^{(L)}(\mathbf{R})$ is represented by a sphere $S^{(L)}$ of radius $|\lambda^{(L)}(\mathbf{R})|$ marked with L pairs of antipodal points. Here, $\lambda^{(7)} = 0$, $\Phi^{(3)}$, $\Phi^{(4)}$, $\Phi^{(6)}$ form an octahedron, a cubic, and an icosahedron. $\Phi^{(5)}$ is a polyhedron with 5 vertices forming a pentagon. The texture of $\Phi_M^{(2)}(x)$ depicted implies a line defect inside loop C , whereas the texture of $\Phi_M^{(1)}(x)$ is defect free. Our model calculations for spin $f = 21/2$ Fermi gas reveal Platonic solid configurations like (c), (d), (f) and dodecahedron (g) in certain parameter regimes.

ments in ^{40}K [5–7], where dipolar interactions are negligible. Many other high spin systems (i.e. ^{161}Dy) have stronger dipolar interactions which will lead to non-uniform spin ordering. As a first step, we shall ignore dipolar interactions. In practice, dipolar interactions can be averaged out to zero through a sequence of magnetic pulses[21]. On the other hand, many competing orders may arise at low temperatures, including the superconducting ordering. Different orders would be favored in different regions in the parameter space. For instance, for spin-1/2 fermions, attractive interaction leads to superconducting phase while repulsive interaction induces magnetic ordering [22]. For higher spin systems, in general, the orders may have overlap in the parameter space and different orders will compete with each other. Here we do not consider the possibility of competing phases, and discuss first the parameter regions that can give rise to spin ordering.

A. Mean Field Phase Diagram

The Hamiltonian for local spin-exchange interaction is $H = H_0 + H_1$, where the kinetic and interaction parts are

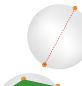
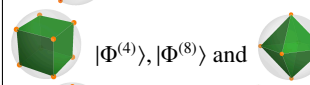
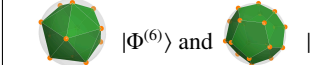
$$H_0 = \int d^3\mathbf{r} \sum_m \psi_m^\dagger(\mathbf{r}) \left(\frac{\hbar^2 \nabla^2}{2\tilde{m}} - \mu \right) \psi_m(\mathbf{r}) \quad (23)$$

$$H_1 = \int d^3\mathbf{r} \sum_{\substack{m_1 m_2 \\ m_3 m_4}} \psi_{m_1}^\dagger(\mathbf{r}) \psi_{m_2}^\dagger(\mathbf{r}) \gamma_{m_1 m_2 m_3 m_4} \psi_{m_4}(\mathbf{r}) \psi_{m_3}(\mathbf{r}), \quad (24)$$

where \tilde{m} is the fermion mass, μ is the chemical potential, and

$$\gamma_{m_1 m_2 m_3 m_4} = \frac{1}{2} \sum_{F=0,2,\dots}^{2f-1} g_F \sum_{M_F=-F}^F \langle m_1 m_2 | F M_F \rangle \langle F M_F | m_3 m_4 \rangle. \quad (25)$$

TABLE I. Exploration of $T = 0$ mean field phase diagram for spin $f = 21/2$ fermion systems in the presence of spin exchange interactions. $k_n = (6\pi^2 n)^{1/3}$, where n is the *total* number of particles in the system. $\{a_F, F = 0, 2, \dots, 2f - 1\}$ are scattering channels with total spin F . The spin orders of different sectors are represented in Majorana representation. $|\Phi^{(L)}\rangle$ sector would contain $2L$ points (L pairs). But different points may occupy the same location, as is the case in (I) and (II). The objects in set (II) and (III) are Platonic solids. All of these states are inert states.

Set	$k_n a_0$	$k_n a_2$	$k_n a_4$	$k_n a_6$	$k_n a_8$	$k_n a_{10}$	$k_n a_{12}$	$k_n a_{14}$	$k_n a_{16}$	$k_n a_{18}$	$k_n a_{20}$	Sectors of Spin Order
(I)	0.1	0.3	0.4	0.45	0.5	0.5	0.45	0.45	-0.3	-0.5	-0.5	 $ \Phi^{(1)}\rangle, \Phi^{(2)}\rangle, \Phi^{(3)}\rangle, \Phi^{(4)}\rangle$
(II)	-0.1	-0.6	-0.6	0.55	0.75	0.75	0.45	-0.75	-0.8	0.8	0.8	 $ \Phi^{(4)}\rangle, \Phi^{(8)}\rangle$ and $ \Phi^{(6)}\rangle$
(III)	-0.6	-0.74	0.87	0.79	0.84	-0.8	-0.83	0.82	0.82	-0.85	0.85	 $ \Phi^{(6)}\rangle$ and $ \Phi^{(10)}\rangle$

Here $\langle m_1 m_2 | F M_F \rangle$ is an abbreviation for Clebsch-Gordon coefficients $\langle f m_1; f m_2 | F M_F \rangle$. $g_F \equiv 4\pi\hbar^2 a_F / \tilde{m}$ is the interaction constant in the scattering channel with total spin- F , and a_F is the corresponding scattering length. For half integer spin

f , $\langle f m_1; f m_2 | F M_F \rangle = \pm \langle f m_2; f m_1 | F M_F \rangle$ for odd/even F respectively. Thus, (24) and Fermi statistics require F to be even integers only. That means $\gamma_{m_1 m_2 m_3 m_4}$ is odd under the exchange $m_1 \leftrightarrow m_2$ or $m_3 \leftrightarrow m_4$.

(It is useful here to summarize our notations. (f, m) are the eigenvalues of single atom spin operators (\mathbf{F}^2, F_z) . (F, M_F) is the total spin and magnetic quantum number when two atoms scatter with each other. (L, M) introduced previously denote the particle-hole total angular momentum quantum numbers, and is the quantum numbers we use to classify spin orders in terms of different sectors $|\Phi^{(L)}\rangle$ in (11).)

We shall study the *uniform* spin order using the mean field approximation. The order parameter is $\rho_{m_1 m_2}$ defined in (1), and it is equal to the average

$$\rho_{m_1 m_2} = \int \frac{d^3 \mathbf{r}}{V} \rho_{m_1 m_2}(\mathbf{r}) = \frac{1}{V} \sum_{\mathbf{k}} \langle c_{\mathbf{k} m_2}^\dagger c_{\mathbf{k} m_1} \rangle, \quad (26)$$

where we used the Fourier transform $\psi_m(\mathbf{r}) = \frac{1}{\sqrt{V}} \sum_{\mathbf{k}} e^{i\mathbf{k}\cdot\mathbf{r}} c_{\mathbf{k} m}$, and V is the volume. Then the mean field Hamiltonian reads $H_{\text{MF}} = \sum_{\mathbf{k}, m_1 m_2} c_{\mathbf{k} m_1}^\dagger \mathcal{H}_{m_1 m_2}(\mathbf{k}) c_{\mathbf{k} m_2}$, with

$$\mathcal{H}_{m_1 m_2}(\mathbf{k}) = (\varepsilon_{\mathbf{k}} - \mu) \delta_{m_1 m_2} + 4\Gamma_{m_1 m_2}, \quad (27)$$

$$\Gamma_{m_1 m_2} = \sum_{m_3 m_4} \gamma_{m_1 m_3 m_2 m_4} \rho_{m_3 m_4}. \quad (28)$$

Here $\varepsilon_{\mathbf{k}} = \hbar^2 k^2 / 2\tilde{m}$ is the kinetic energy. The quadratic Hamiltonian can be diagonalized in spin space through a unitary transform $(U^\dagger \mathcal{H}(\mathbf{k}) U)_{m_1 m_2} = (\varepsilon_{\mathbf{k}} - \mu_{m_1}[\Gamma]) \delta_{m_1 m_2}$, where $\mu_m[\Gamma] = \mu - 4(U^\dagger \Gamma U)_{mm}$. Then the quasi-particles $b_{\mathbf{k} m_1} = \sum_{m_2} U_{m_1 m_2}^\dagger c_{\mathbf{k} m_2}$ are free fermions obeying $\frac{1}{V} \sum_{\mathbf{k}} \langle b_{\mathbf{k} m_1}^\dagger b_{\mathbf{k} m_2} \rangle = n_{m_1} \delta_{m_1 m_2}$, where $n_{m_1} = \frac{1}{V} \sum_{\mathbf{k}} \left(e^{(\varepsilon_{\mathbf{k}} - \mu_{m_1}[\Gamma]) / k_B T} + 1 \right)^{-1}$. With the above information, we can determine the order parameter through the consistency equation

$$\rho_{m_1 m_2} = \sum_{m_3} U_{m_1 m_3} n_{m_3} U_{m_3 m_2}^\dagger, \quad (29)$$

and obtain the spinor vectors $\{\Phi^{(L)}\}$ using Eqn.(8).

We have solved the self consistency equation (29) at $T = 0$ numerically for the case of $f = 21/2$ with some specific value of gas parameters $\{k_n a_F\}$'s, where

$$k_n = (6\pi^2 n)^{1/3}, \quad (30)$$

and n is the total number density. See Table I. Since a_F 's are unknown at present, we have tried various parameter sets, labelled (I) to (III) in Table I. Their mean field states are:

(I): Only $\Phi^{(1)}, \Phi^{(2)}, \Phi^{(3)}, \Phi^{(4)}$ are nonzero. The Majorana points of each one of them collapse into a single antipodal pair like (a) and (b) in Fig. 1. The pairs of different L orient differently.

(II): Only $\Phi^{(4)}, \Phi^{(6)}, \Phi^{(8)}$ are non-zero. $\Phi^{(4)}$ and $\Phi^{(8)}$ form cubes (Fig.1(d)). $\Phi^{(6)}$ forms an octahedron (Fig.1(c)). For $\Phi^{(8)}$ and $\Phi^{(6)}$, the vertices of the cube and octahedron are doubly occupied respectively.

(III): Only $\Phi^{(6)}$ and $\Phi^{(10)}$ are non-zero. $\Phi^{(6)}$ forms an isocahedron (Fig.1(f)) and $\Phi^{(10)}$ forms a dodecahedron (Fig.1(g)).

The states found in (II) and (III) are the Platonic solids. All the states in (I) to (III) are the so-called inert states as the distances between Majorana points in these states are independent of interactions. All these states are found in a region containing the parameter set in Table I. There are also non-inert state in other regions of parameter space.

B. Mean field phase boundary

Since there are many scattering parameters $\{a_F, F = 0, 2, \dots, 2f\}$ for large spin systems, it is laborious to explore every corner in the phase diagram numerically. However, considerable insight can be gained by exploring the phase transition boundary using Ginzburg-Landau theory.

Near the phase boundary, the spin order $\tilde{\rho}_{m_1 m_2}$ defined in Eqn.(15) is small. We can then expand the free energy in

mean field approximation

$$\Omega = -\frac{1}{\beta} \ln(\text{Tr} e^{-\beta H_{\text{MF}}}) - B \quad (31)$$

around $\tilde{\rho}_{m_1 m_2} = 0$, where $\beta = 1/k_B T$ is the inverse temperature. Here $H_{\text{MF}} = H_{\text{MF}}^{(0)} + H_{\text{MF}}^{(1)}$, with

$$H_{\text{MF}}^{(0)} = \sum_{\mathbf{k}m} (\epsilon_{\mathbf{k}} - \mu) c_{\mathbf{k}m}^\dagger c_{\mathbf{k}m}, \quad (32)$$

$$H_{\text{MF}}^{(1)} = \sum_{\mathbf{k}m_1 m_2} \tilde{\Gamma}_{m_1 m_2} c_{\mathbf{k}m_1}^\dagger c_{\mathbf{k}m_2}, \quad (33)$$

$$\tilde{\Gamma}_{m_1 m_2} = 4 \sum_{m_3 m_4} \gamma_{m_1 m_3 m_2 m_4} \tilde{\rho}_{m_3 m_4}, \quad (34)$$

and we have restored the condensate energy $B = \langle H - H_{\text{MF}} \rangle_{\text{MF}}$ to the free energy,

$$\begin{aligned} B &= 2V \sum_{m_1 \dots m_4} \gamma_{m_1 m_2 m_3 m_4} \rho_{m_3 m_1} \rho_{m_4 m_2} \\ &= 2V \sum_{m_1 m_2} \tilde{\Gamma}_{m_1 m_2} \tilde{\rho}_{m_2 m_1} + Vn^2 \sum_{F=0,2,\dots}^{2f-1} g_F \frac{2F+1}{(2f+1)^2}. \end{aligned} \quad (35)$$

Terms linear in $\tilde{\rho}_{m_1 m_2}$ vanishes due to the identity

$$\langle f m_1; f m_2 | F M_F \rangle = (-1)^{f+m_2} \sqrt{\frac{2F+1}{2f+1}} \langle f(-m_2); F M_F | f m_1 \rangle \quad (36)$$

and completeness relation $1 = \sum_m |f m\rangle \langle f m|$. Similarly, one can show that $\tilde{\Gamma}_{m_1 m_2}$ is traceless and Hermitian.

Using the technique of linked cluster expansion [23], we have

$$\begin{aligned} \Omega &= \Omega_0 - B - \frac{1}{\beta} \sum_{l=1}^{\infty} M_l, \quad \Omega_0 = -\frac{1}{\beta} \ln \text{Tr} e^{-\beta H_{\text{MF}}^{(0)}}, \quad (37) \\ M_l &= \frac{(-1)^l}{l!} \int_0^\beta d\tau_1 \dots \int_0^\beta d\tau_l \langle \mathcal{T}_\tau H_{\text{MF}}^{(1)}(\tau_1) \dots H_{\text{MF}}^{(1)}(\tau_l) \rangle_c, \end{aligned} \quad (38)$$

where $H_{\text{MF}}^{(1)}(\tau) = e^{\tau H_0} V e^{-\tau H_0}$, and “ $\langle \dots \rangle_c$ ” means connected diagrams, \mathcal{T}_τ is the imaginary-time ordering. Evaluating (38) using Wick's theorem and keeping up to second order in $\tilde{\rho}_{m_1 m_2}$, we have

$$\Delta\Omega = -\frac{V}{2} (\text{Tr} \tilde{\rho} + \chi(T, \mu) \text{Tr} \tilde{\rho}^2), \quad (39)$$

where we have treated $\tilde{\Gamma}_{m_1 m_2}$ and $\tilde{\rho}_{m_1 m_2}$ as matrices. The susceptibility function is

$$\chi(T, \mu) = \frac{1}{T} \sum_{\mathbf{k}} f_{\mathbf{k}} (1 - f_{\mathbf{k}}) = \int_0^\infty d\varepsilon D(\varepsilon) \left(-\frac{\partial f(\varepsilon)}{\partial \varepsilon} \right), \quad (40)$$

where $D(\varepsilon) = 3n \sqrt{\varepsilon} / 2\varepsilon_n^{3/2}$ is the density of states, $\varepsilon_n = \hbar^2 k_n^2 / 2\tilde{m}$, and $f_{\mathbf{k}} = (e^{(\varepsilon_{\mathbf{k}} - \mu)/T} + 1)^{-1}$ is the Fermi distribution function. $\chi(T, \mu)$ is always positive and increases as temperature is lowered.

Now we express (39) in terms of $\Phi_M^{(L)}$ to see the emergence of each L -sector of the spin order. Note that $\tilde{\rho}_{m_1 m_2}$ has the

same expansion as those of $\rho_{m_1 m_2}$ in equation (6), except for the absence of $L = 0$ term. Combined with (34), we have

$$\tilde{\Gamma}_{m_1 m_2} = - \sum_{L=1}^{2f} \sum_{M=-L}^L \Phi_M^{(L)} G_L (\mathcal{Y}_M^{(L)})_{m_1 m_2}, \quad (41)$$

$$G_L = 2 \sum_{F=0,2,\dots}^{2f-1} g_F (2F+1) W(FL). \quad (42)$$

Here we used the identity

$$\begin{aligned} &\sum_{m_1 m_2 M_F} \langle F M_F | f m_1; f m_a \rangle \langle f m_1 | L M; f m_2 \rangle \langle f m_2; f m_b | F M_F \rangle \\ &= \langle s m_b | L M; s m_a \rangle (-1)^{2f-F} (2F+1) W(FL), \end{aligned} \quad (43)$$

which is derived from the definition of Racah coefficients $W(f f f f; FL) \equiv W(FL)$ [12]. Feeding the expansions into (39), we reach the concise form

$$\Delta\Omega = \frac{n^2 V}{2} \sum_{L=1}^{2f} \sum_{M=-L}^L |\Phi_M^{(L)}|^2 G_L [1 - \chi(T, \mu) G_L]. \quad (44)$$

Equation(44) shows that $\Phi^{(L)}$ will emerge if

$$(i) \quad G_L > 0, \quad \text{and} \quad (ii) \quad \chi G_L \geq 1, \quad (45)$$

where the equal sign gives the phase boundary. Up to the quadratic order in $\Phi_M^{(L)}$, all M components are degenerate. Higher order terms in $\Phi^{(L)}$ will lift the degeneracy and mix different L components. Condition (i) is necessary for the ordered phase to be stable. Consider a single $\Phi_M^{(L)}$, which means $\tilde{\Gamma} = -G_L \Phi_M^{(L)} \mathcal{Y}_M^{(L)}$. Then for the ordering to be stable, the energy B in Eqn.(35) must be lowered due to the presence of spin orders $\Phi_M^{(L)}$. Since $B = -2V(\Phi_M^{(L)} \mathcal{Y}_M^{(L)})^2 G_L + \text{constant}$, the case $G_L > 0$ will ensure the spin ordered phase is energetically favored over the normal phase. Condition (ii) simply means that the spin-ordered state is at least a local minimum in the free energy functional.

To help further understanding the conditions (45), consider a spin-1/2 systems. Here the only non-trivial spin order is $L = 1$ ferromagnetic ordering, and $G_1 = g_0$. Then condition (i) reduces to $g_0 > 0$, which means the interactions are repulsive. Condition (ii) $\chi g_0 \geq 1$ is the Stoner criterion for ferromagnetic ordering. (Note $\chi \rightarrow D(\varepsilon_F)$ at $T = 0$). For higher spin systems, G_L represents the total interaction strength responsible for triggering the spin order $|\Phi^{(L)}\rangle$. Since the Racah coefficients $W(FL)$ can be both positive and negative, not all g_F 's have to be repulsive in order to create a critical total interaction G_L to start the spin order, unlike the spin-1/2 case.

Experimental parameters are usually expressed by scattering length a_F . Thus, we define the total scattering length A_L

$$G_L = \frac{8\pi\hbar^2 A_L}{\tilde{m}}, \quad A_L = \sum_F a_F (2F+1) W(F, L). \quad (46)$$

Next, we note that $\chi(T, \mu)$ in Eqn.(40) has the dimension of density of state. It scales as $\sqrt{\mu}$ and hence represents a momentum scale. We can then define a wavevector $k(T, \mu)$ as

$\chi(T, \mu) = (\tilde{m}/2\pi^2\hbar^2)k(T, \mu)$. (Note that $k(0, \mu) = k_n$). Condition (ii) then becomes

$$k(T, \mu)A_L \geq \frac{\pi}{4}, \quad \text{or} \quad k_n A_L \geq \frac{\pi}{4} \frac{k_n}{k(T, \mu)}, \quad (47)$$

where the equal sign gives the phase boundary.

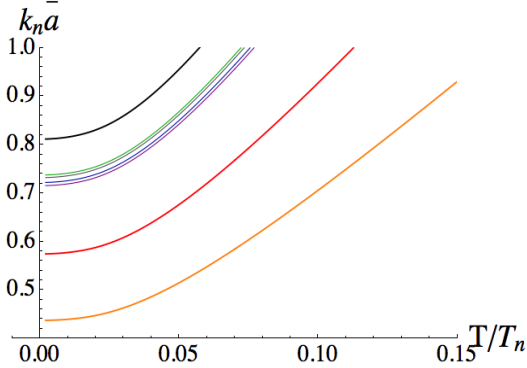


FIG. 2. The transition temperature for spin order $|\Phi^{(L)}\rangle$ for $L = 1, 2, 6, 3, 5, 4, 7$, (from bottom to top), for a spin $f = 21/2$ Fermi gas.

Certainly, the larger the A_L , the easier for the L -th spin order to emerge. However, for small gas parameters $k_n a_F < 1$, it is not clear whether Eq.(47) can be satisfied. On the other hand, one sees from equation (46) that A_L will be maximized if the sign of a_F matches that of the Racah coefficient $W(F, L)$. To demonstrate this effect, we consider a set of a_F 's with the same magnitude \bar{a} with a sign matching that of $W(F, L)$. equation (47) then becomes

$$k_n \bar{a} \geq \frac{\pi/4}{\sum_{F=0,2,\dots}^{2f} (2F+1)|W(F, L)|} \frac{k_n}{k(T, \mu)}. \quad (48)$$

This condition is plotted in Figure 2 for a spin $f = 21/2$ Fermi gas. It shows spin orders as high as $L = 7$ can emerge at the phase boundary for $k_n \bar{a} < 1$. While equation (48) is sufficient

for the appearance of $\Phi^{(L)}$, it is not necessary. Once a low order $\Phi^{(L)}$ is present, say, $L = 1$, higher L spin order can emerge through non-linear coupling as temperature is lowered. Finally, we note from Eqn.(48) that the larger the spin f of the fermions, the larger the sum in Eqn.(48), and the smaller the gas parameter $k_n \bar{a}$ needed to activate the spin order.

V. EXPERIMENTAL DETERMINATION OF THE DENSITY MATRIX

Since the diagonal element of the density matrix is the spin population along a specified spin quantization axis, say \hat{z} , they can be determined by the Stern-Gerlach method. To access the off diagonal elements, one can apply a magnetic pulse to rotate ρ to $\rho' = D\rho D^\dagger$, where D is a rotational matrix, see Eqn.(3). The diagonal elements of ρ' will then contain information of the off-diagonal elements of ρ due to the rotation D . By repeating the measurement of diagonal matrix elements for different D 's, one can then extract the information of the off-diagonal matrix elements of the original density matrix ρ .

VI. CONCLUDING REMARKS

Large spin quantum gases are fertile grounds for new quantum matter. Here, we have pointed out the very rich spin order possible in large spin fermions, most of which have no analog in electron matters. We show that the spin order in different sectors can be conveniently described as Majorana antipodal points on a sequence of spheres representing the spin order of different particle-hole angular momenta. Our model calculations show that some of these orders can take the form of Platonic solids, which are structures that exist within certain *region* of the parameter space instead of a single point. These structures are therefore robust and will have good chance to be realized.

ACKNOWLEDGEMENTS

This work is supported by DARPA under the Army Research Office Grant Nos. W911NF-07-1-0464, W911NF0710576, and NSF Grant DMR-1309615.

-
- [1] M. Lu, N. Q. Burdick, S. H. Youn, B. L. Lev, Phys. Rev. Lett. **107**, 190401 (2011).
 - [2] M. Lu, N. Q. Burdick, B. L. Lev, Phys. Rev. Lett. **108**, 215301 (2012).
 - [3] T. L. Ho, Phys. Rev. Lett. **81**, 742 (1998); T. Ohmi and K. Machida, J. Phys. Soc. Jpn. **67**, 1822 (1998).
 - [4] T. L. Ho and S. K. Yip, Phys. Rev. Lett. **82**, 247 (1999).
 - [5] J. S. Krauser, J. Heinze, N. Flschner, S. Gtze, O. Jrgensen, D.-S. Lhmann, C. Becker, K. Sengstock, Nat. Phys. **8**, 813 (2012)
 - [6] J. Heinze, J. S. Krauser, N. Flschner, K. Sengstock, C. Becker, U. Ebling, A. Eckardt, M. Lewenstein, *et. al.*, Phys. Rev. Lett. **110**, 250402 (2013).
 - [7] J. S. Krauser, U. Ebling, N. Flschner, J. Heinze, K. Sengstock, M. Lewenstein, A. Eckardt, C. Becker, Science **343**, 157 (2014).
 - [8] C. Wu, J.-P. Hu, S.-C. Zhang, Phys. Rev. Lett. **91**, 186402 (2003).
 - [9] A. V. Gorshkov, M. Hermele, V. Gurarie, C. Xu, P. S. Julienne, J. Ye, P. Zoller, E. Demler, M. D. Lukin, A. M. Rey, Nat. Phys. **6**, 289 (2010).
 - [10] J. Jaramillo, S. Greschner, T. Vekua, Phys. Rev. A **88**, 043616 (2013).
 - [11] H. Makela and K.-A. Suominen, Phys. Rev. Lett. **99**, 190408 (2007).
 - [12] D. M. Brink and G. R. Satchler, *Angular Momentum* 2ed, Clarendon Press, Oxford (1968).
 - [13] E. Majorana, Nuovo Cimento **9**, 43 (1932).

- [14] R. Barnett, A. Turner, and E. Demler, Phys. Rev. Lett. **97**, 180412 (2006).
- [15] A. Lamacraft, Phys. Rev. B **81**, 184526 (2010); Y. Kawaguchi, and M. Ueda, Phys. Rev. A **84**, 053616 (2011); M. Fizia, and K. Sacha, J. Phys. A: Math. Theor. **45**, 045103 (2012); H. Makela, and K.-A. Suominen, Phys. Rev. Lett. **99**, 190408 (2007); R. Barnett, D. Podolsky, and G. Refael, Phys. Rev. B **80**, 024420 (2009).
- [16] J. J. Sakurai and J. Napolitano, *Modern Quantum Mechanics* 2nd edition, Addison Wesley (2010) pp. 232-238.
- [17] H. Mäkelä and K.-A. Suominen, Phys. Rev. Lett. **99**, 190408 (2007).
- [18] $|\Psi^{(1)}\rangle = \lambda(-\frac{1}{2}\sin\theta e^{-i\phi} a^{\dagger 2} + \cos\theta a^{\dagger} b^{\dagger} + \frac{1}{2}\sin\theta e^{i\phi} b^{\dagger 2})|0\rangle$. $|\Phi^{(1)}\rangle \rightarrow -|\Phi^{(1)}\rangle$ as $\theta \rightarrow \pi - \theta$, $\phi \rightarrow \phi + \pi$.
- [19] The system has two distinct antipodal pairs, $[\hat{\mathbf{n}}]$ and $[\hat{\mathbf{m}}]$. Choosing the z -axis along $\hat{\mathbf{n}} \times \hat{\mathbf{m}}$, the polar angles of $\hat{\mathbf{n}}$ and $\hat{\mathbf{m}}$ are $(\pi/2, \phi_1)$ and $(\pi/2, \phi_2)$ respectively. The corresponding quantum state is $|\Phi^{(2)}\rangle = \frac{1}{4}(-e^{-i\phi_1} a^{\dagger 2} + e^{i\phi_1} b^{\dagger 2})(-e^{-i\phi_2} a^{\dagger 2} + e^{i\phi_2} b^{\dagger 2})|0\rangle$, which is unchanged under a π -rotation about $\hat{\mathbf{z}}$, which changes ϕ_i to $\phi_i + \pi$. Next, if we choose the z -axis along $\hat{\mathbf{n}} + \hat{\mathbf{m}}$, and the x -axis along $\hat{\mathbf{n}} - \hat{\mathbf{m}}$, the polar angles of $\hat{\mathbf{n}}$ and $\hat{\mathbf{m}}$ are then $(\theta, 0)$ and (θ, π) respectively. The corresponding state is $|\Phi^{(2)}\rangle = \frac{1}{4}(-\sin\theta[a^{\dagger 2} + b^{\dagger}] + 2\cos\theta a^{\dagger} b^{\dagger}) (\sin\theta[a^{\dagger 2} + b^{\dagger}] + 2\cos\theta a^{\dagger} b^{\dagger})|0\rangle$. This state is also invariant under a rotation of π about $\hat{\mathbf{z}}$, which changes a^{\dagger} to $-ia^{\dagger}$, b^{\dagger} to ib^{\dagger} .
- [20] N. D. Mermin, Rev. Mod. Phys. **51**, 591 (1979).
- [21] M. Vengalattore, S.R. Leslie, J. Guzman, D.M. Stamper-Kurn, Phys. Rev. Lett. **100**, 170403 (2008).
- [22] W. Zwerger, *The BCS-BEC Crossover and the Unitary Fermi Gas*, Springer (2012); A. Auerbach, *Interacting Electrons and Quantum Magnetism*, Springer (2012).
- [23] A. A. Abrikosov, L. P. Gorkov and I. E. Dzyaloshinski, *Methods of Quantum Field Theory in Statistical Physics* (Dover, New York, 1975).